Control Surface Spanwise Placement In Active Flutter Suppression Systems

E.Nissim[1]
NRC-NASA Research Associate
NASA Ames-Dryden Flight Research Facility

J.J.Burken
NASA-Ames-Dryden Flight Research Facility

[1]On leave from Technion-I.I.T.;Haifa,Israel

1 INTRODUCTION

All flutter suppression systems require sensors to detect the movement of the lifting surface and to activate a control surface according to a synthesized control law. Most of the work performed to date (refs. 1 through 5) relate to the development of control laws based on predetermined locations of sensors and control surfaces. These locations of sensors and control surfaces are determined either arbitrarily, or by means of a trial and error procedure (ref. 5)

The aerodynamic energy concept (ref. 6) indicates that the sensors should be located within the activated strip. Furthermore, the best chordwise location of a sensor activating a T.E. control surface, is around the 65-percent chord location (ref. 7). The best chordwise location for a sensor activating a L.E. surface is shown to lie upstream of the wing (around 20-percent upstream of the leading edge), or alternatively, two sensors located along the same chord should be used.

Plan View of a Wing with Active Control Surfaces and Recommended Sensor Locations

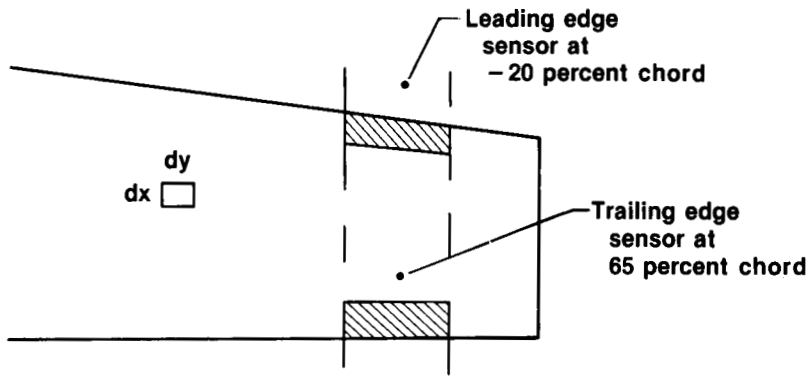

The present work describes a method which enables one to determine the best spanwise placement of an activated control surface without resorting to any specific control law. The method is based on the aerodynamic energy concept whereby the activated control surface is placed at the location where most energy is fed into the unstable structure.

2 APPROACH

Let the pressure $p(x,y)$ be given by eq.(1) and let the displacement $z(x,y)$ be given by eq.(2),where the q's denote the generalized coordinates of the system. The generalized aerodynamic forces per unit area are given by eq.(3), or in a more condensed form by eq.(4).

$$p(x,y) = \begin{bmatrix} p_1(x,y) & p_2(x,y) & \cdots & p_n(x,y) \end{bmatrix} \begin{Bmatrix} q_1 \\ q_2 \\ \vdots \\ q_n \end{Bmatrix} \tag{1}$$

$$z(x,y) = \begin{bmatrix} z_1(x,y) & z_2(x,y) & \cdots & z_n(x,y) \end{bmatrix} \begin{Bmatrix} q_1 \\ q_2 \\ \vdots \\ q_n \end{Bmatrix} \tag{2}$$

$$\{Q\}_{x,y} = \left[\begin{Bmatrix} z_1(x,y) \\ z_2(x,y) \\ \vdots \\ z_n(x,y) \end{Bmatrix} \begin{bmatrix} p_1(x,y) & p_2(x,y) & \cdots & p_n(x,y) \end{bmatrix} \right] \begin{Bmatrix} q_1 \\ q_2 \\ \vdots \\ q_n \end{Bmatrix} \tag{3}$$

$$\{Q\}_{x,y} = [A]_{x,y} \{q\} \tag{4}$$

The work per unit area $W_{x,y}$ done by the system on its surroundings per cycle of oscillation is given by (ref. 6) eq.(5), where eq.(6) provides a definition for some of the parameters in eq.(5). If $W_{x,y} > 0$, energy is dissipated by the system. If $W_{x,y} < 0$, energy is fed into the system. Eq.(8) is obtained by integrating eq.(5) along the chord,and it yields the work W_y per unit span done by the system on its surroundings per cycle of oscillation. The total work W is obtained by integrating eq.(8) along the span, as shown in eqs.(10),(11).

$$W_{x,y} = \frac{\pi}{2} \lfloor q_0^* \rfloor \left(- \left[A_I + A_I^T \right]_{x,y} + i \left[A_R - A_R^T \right]_{x,y} \right) \{q_0\} \tag{5}$$

$$[A]_{x,y} = [A_R]_{x,y} + i\,[A_I]_{x,y} \tag{6}$$

$$W_y = \int_{L.E.}^{T.E.} W_{x,y}\, dx \tag{7}$$

$$W_y = \frac{\pi}{2} \lfloor q_0^* \rfloor \left(- \left[A_I + A_I^T \right]_{y} + i \left[A_R - A_R^T \right]_{y} \right) \{q_0\} \tag{8}$$

$$[A]_y = \int_{L.E.}^{T.E.} [A]_{x,y}\, dx \tag{9}$$

$$W = \int_{-s}^{s} W_y\, dy \tag{10}$$

$$W = \frac{\pi}{2} \lfloor q_0^* \rfloor \left(- \left[A_I + A_I^T \right] + i \left[A_R - A_R^T \right] \right) \{q_0\} \tag{11}$$

$$[A] = \int_{-s}^{s} [A]_y\, dy \tag{12}$$

Define the specific energy ratio by $\overline{\overline{W}}_A$, as given by eq.(13), and note that its integral along the span must have a unit absolute value (see eq.(14)).

$$\overline{\overline{W}}_A = \frac{W_y}{|W|} \tag{13}$$

$$\int_{-s}^{s} \overline{\overline{W}}_A \, dy = \pm 1 \tag{14}$$

It is argued that the best spanwise placement of an active control surface for flutter suppression is around the location where $\overline{\overline{W}}_A$ is negative and assumes the largest numerical values.

3 DETAILED PROCEDURE

1. Determine the flutter dynamic pressure Q_F of the system
2. Increase Q_D,so as to lie within the unstable region, and obtain the eigenvector $\{q_0\}$ of the unstable mode. The amount by which Q_D is increased is immaterial since only energy ratios are used.
3. Compute W (which must be negative),and $\overline{\overline{W}}_A$ for the different spanwise locations.
4. Plot the specific energy ratio $\overline{\overline{W}}_A$ versus the span and determine the strip where $\overline{\overline{W}}_A$ assumes the largest negative value. This strip absorbs most energy per unit span and therefore would present the location where an active control surface would be most effective in suppressing flutter.

4 NUMERICAL EXAMPLES

Three numerical examples are used.These examples relate to

1. DAST-ARW2,12 modes (2 rigid body modes),see ref. 8.
2. OBLIQUE WING,20 modes(5 rigid body modes),see ref. 9.
3. MODIFIED OBLIQUE WING (with one torsional modal frequency reduced so as to cause wing flutter)

The relevant aerodynamic matrices were computed using Langley's doublet lattice ISAC program.The results obtained are shown in the following figures.

Oblique Wing Model Planform View with Wing Skewed 65°

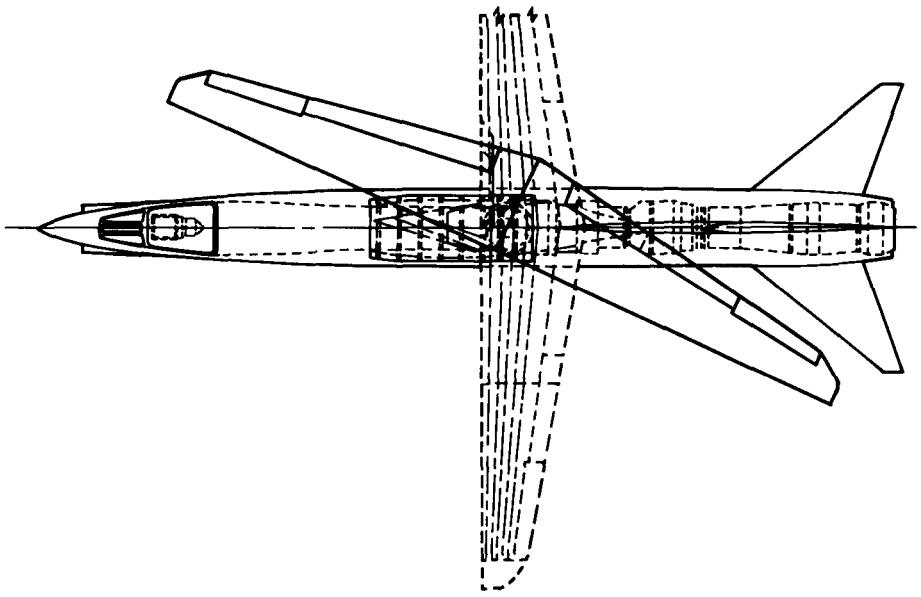

5 Results for the DAST-ARW2 Mathematical Model

The geometrical layout of the DAST-ARW2 model is shown below. It can be seen that out of the 24 strips allowed for the model,17 strips lie along the wing, 4 strips lie along vertical tail and 3 strips lie along the horizontal tail. This model yields a flutter dynamic pressure $Q_F = 490psf$ (at M=0.85) and a flutter frequency $\omega_F = 117rad/s$. The unstable eigenvector was computed for $Q = 550psf$ and the matrices $[A]$ and $[A]_y$ were computed for all the 24 strips at the reduced frequency $k = 0.132$ associated with the unstable mode.

ARW2 Geometric Layout, Together with Doublet Lattice Paneling and Strip Number Allocations

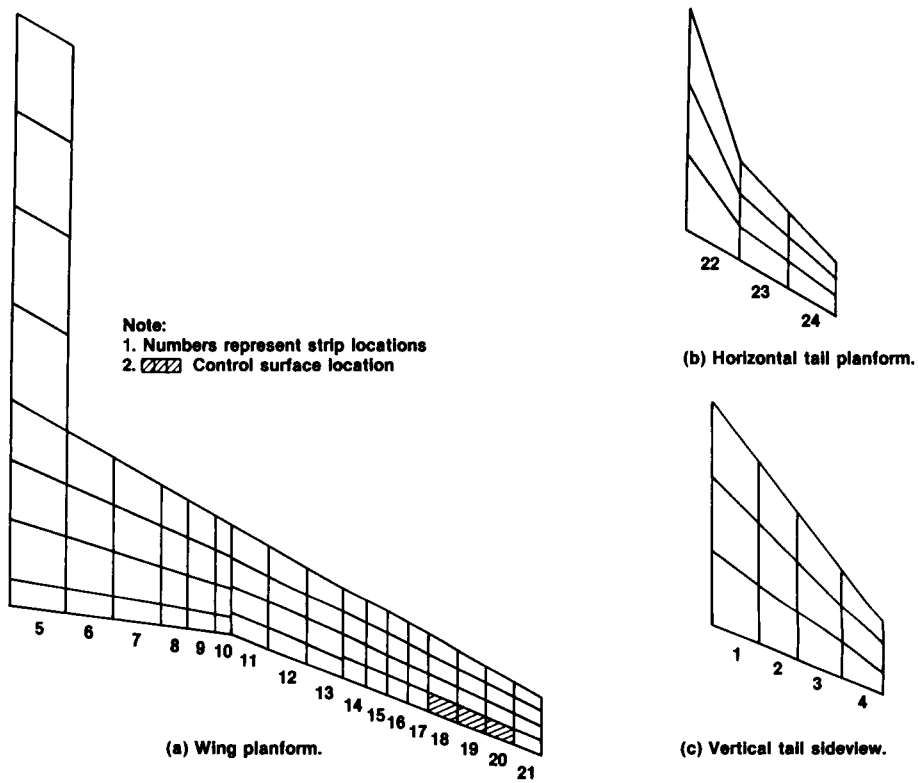

The figure below shows a plot of the specific energy ratios $\overline{\overline{W}}_A$ for only those 17 strips that lie along the wing. The values of $\overline{\overline{W}}_A$ are negligible for all the other strips and therefore will not be shown herein. As can be seen, the specific energy ratio is negative for all wing strips, except for the root strip (strip 5) where $\overline{\overline{W}}_A$ is very small and positive. The largest negative numerical value of $\overline{\overline{W}}_A$ relates to strip 18, which coincides with the inboard portion of the aileron. Following the method described herein, this is the location around which the aileron should be placed for best effects regarding flutter suppression (i.e. around the 80-percent span location).

DAST – ARW2 Model – Variation of Specific Energy Ratio $\overline{\overline{W}}_A$ with Strip Locations Along the Wing

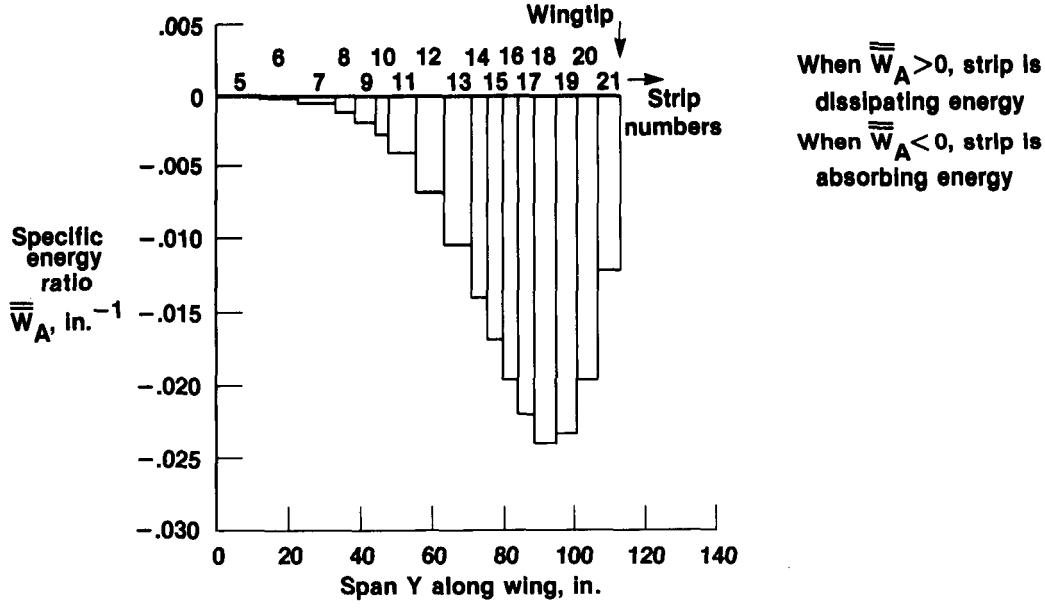

6 Results for the Oblique Wing

The geometrical layout of the wing in a 65-degrees skew position (with right wing forward) is shown. Note that the wing has again 17 strips along its span,with strip 6 at the tip of the left wing and strip 22 at the tip of the right wing.

Oblique Wing Model – Geometric Layout Together with Doublet Lattice Paneling and Strip Numbers
Planeform 65° Skew

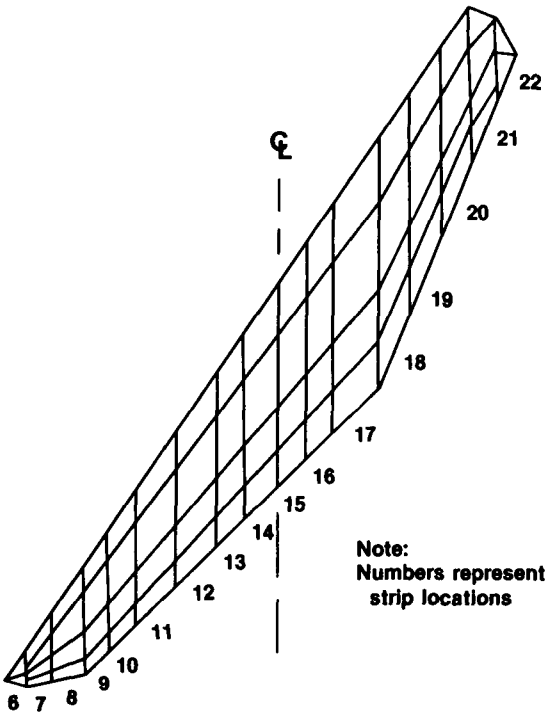

The horizontal tail, the horizontal projection of the fuselage, and the side view of the vertical tail are both shown in the figure below. There are 4 strips on each of the horizontal tails (left and right surfaces), 2 strips on the horizontal projection of the fuselage, and 4 strips on the vertical tail.

A flutter computation at Mach 0.95 shows that a mild, 78 rad/s, vertical tail flutter instability develops around $Q_F = 780psf$.

Oblique Wing Model – Geometric Layout Together with Doublet Lattice Paneling and Strip Numbers

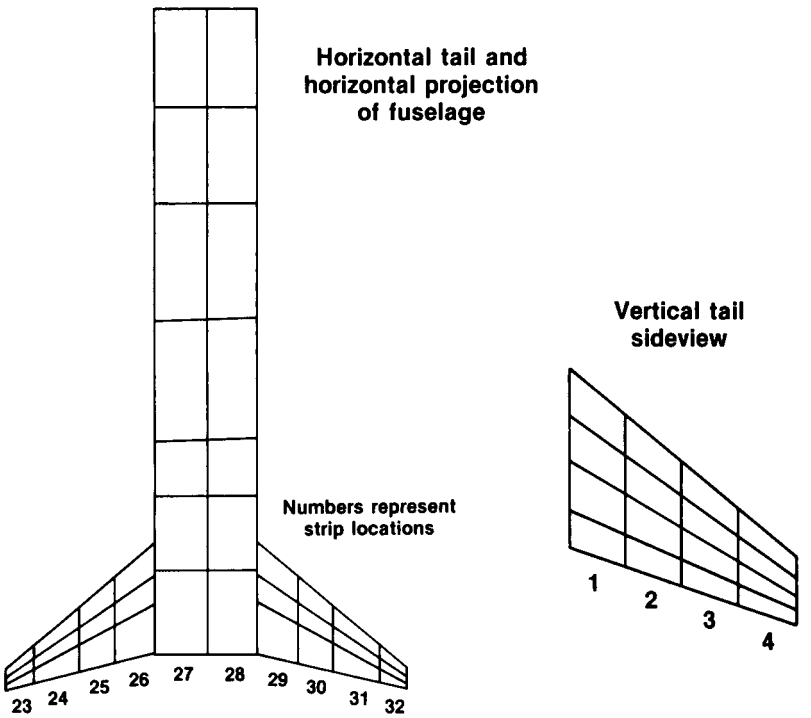

The specific energy ratio distribution was computed for Q=1600 psf. It can be seen that most of the energy input into this fluttering system takes place through the vertical tail and the tips of the horizontal tail. The inboard parts of the horizontal tail, the horizontal fuselage, and practically all of the wing,all dissipate energy and thus contribute to the mildness of the flutter obtained. The following figures indicate that for the suppression of this flutter mode, the active control surface should be placed around the center of strip 3 of the vertical tail (i.e. around its 60-percent span location).

Oblique Wing Model – Variation of Specific Energy Ratio $\overline{\overline{W}}_A$ with Strip Locations

Wing

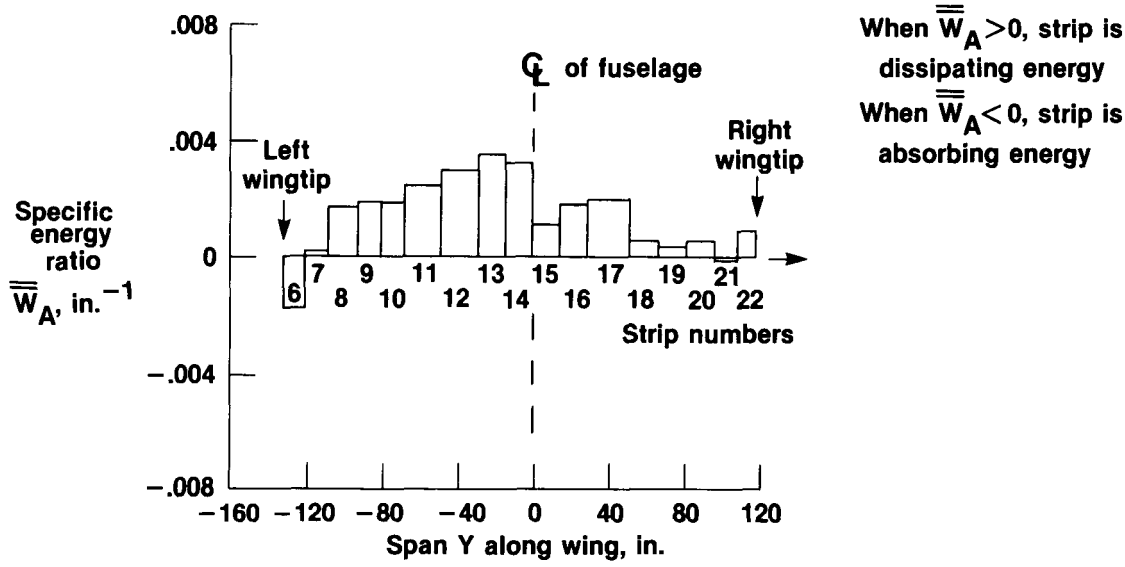

Oblique Wing Model – Variation of Specific Energy Ratio $\overline{\overline{W}}_A$ with Strip Locations

Horizontal Tail and Horizontal Fuselage

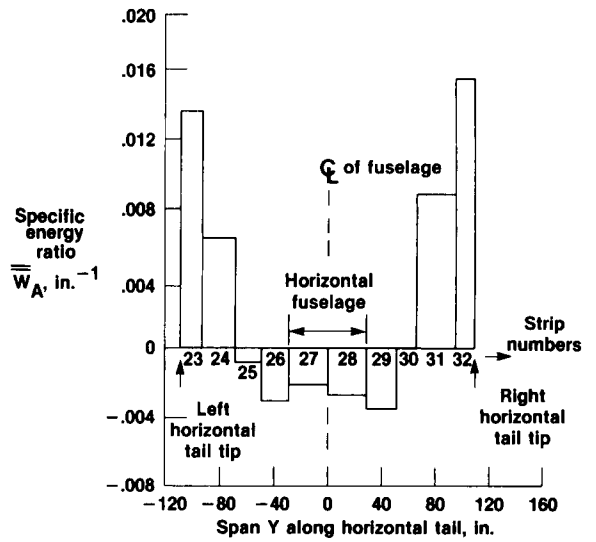

Oblique Wing Model – Variation of Specific Energy Ratio $\overline{\overline{W}}_A$ with Strip Locations

Vertical Tail

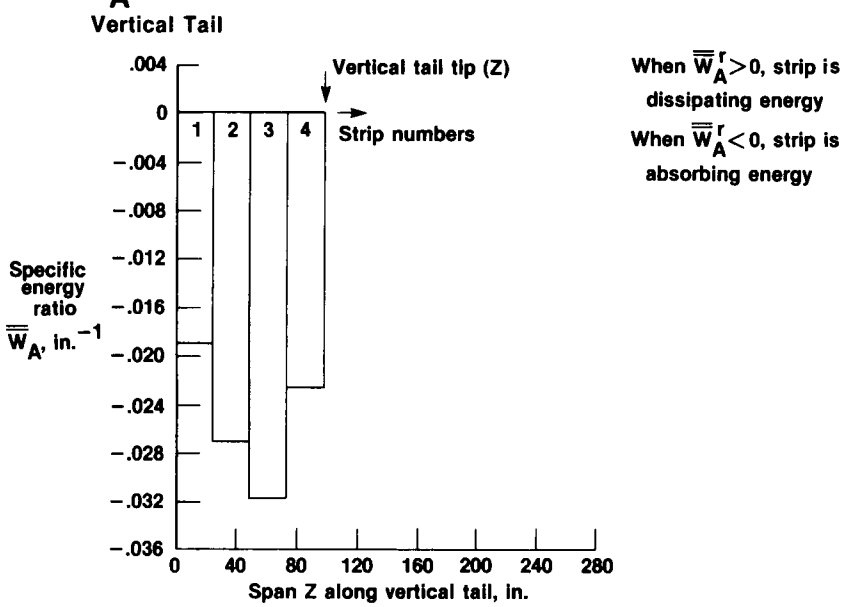

7 Results for the Modified Oblique Wing

The oblique wing is unique from the point of view of assymetry. The best placement of an activated strip along its span could present an interesting challenge. The mathematical model of the wing was therefore modified so as to 'force' the wing to flutter. This was done by lowering one of the torsional frequencies of the wing from 45 HZ to 12 HZ. Therefore, the following results do not relate to the actual wing but to a synthetically modified wing. This modified model yields,in addition to the already seen vertical tail flutter,a wing flutter mode with $Q_F = 1050psf$ and $\omega_F = 70rad/s$. The following results relate to this wing flutter mode, with specific energy ratios computed at Q=1300 psf.

Modified Oblique Wing Model – Variation of Specific Energy Ratio $\overline{\overline{W}}_A$ with Strip Locations

Horizontal Tail and Horizontal Fuselage

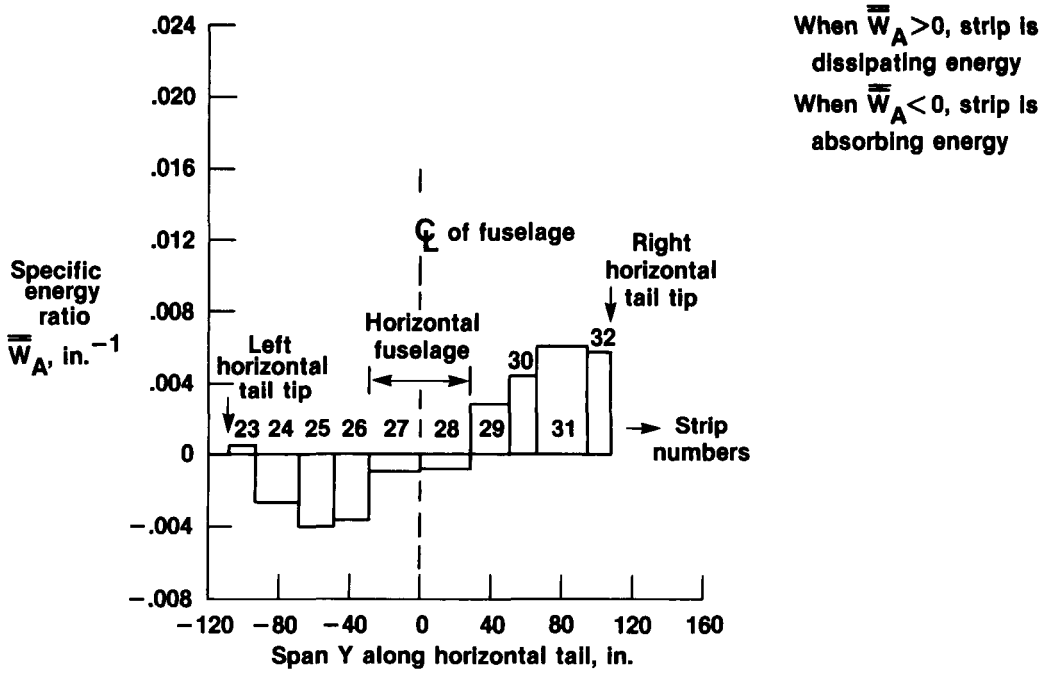

Modified Oblique Wing Model – Variation of Specific Energy Ratio $\overline{\overline{W}}_A$ with Strip Locations

Vertical Tail

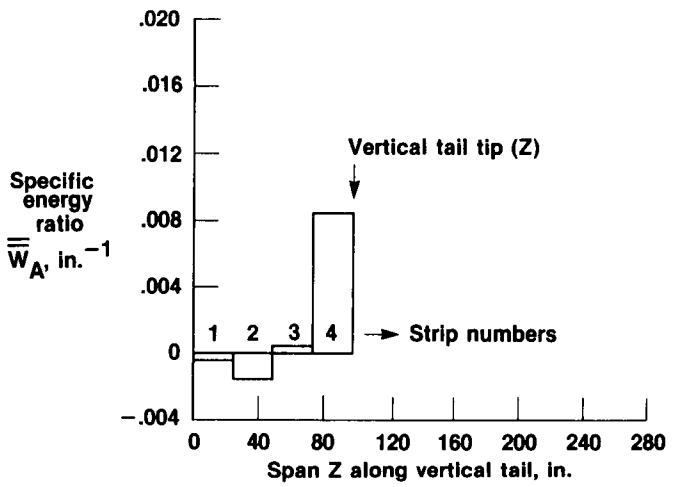

Modified Oblique Wing Model – Variation of Specific Energy Ratio $\overline{\overline{W}}_A$ with Strip Locations

Wing

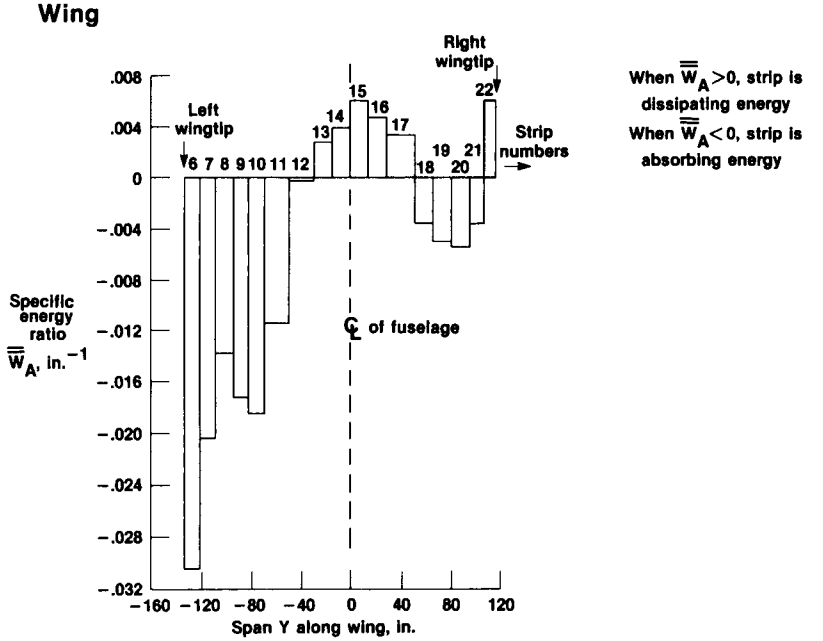

As seen from the above 3 figures,most of the energy input into the system takes place through the left wing. The vertical tail essentially dissipates energy, and the horizontal tail absorbs energy through its left surface and dissipates around the same amount of energy through its right surface. The largest negative numerical value for $\overline{\overline{W}}_A$ is obtained in strip 6 which represents the tip of the left (aft) wing. Hence, for the suppression of this flutter mode, the activated control surface should be placed as close to the left tip of the wing as is structurally possible. Strips 9 and 10 can also form a reasonable alternative to the above extreme tip placement of the activated control surface,i.e.,around the 65-percent span location of the left wing.

8 REFERENCES

1. Newsom, J.R.: A Method For Obtaining Practical Flutter Suppression Control Laws Using Results of Optimal Control Theory. NASA TP-1471,1979.

2. Mukhopadhyay, V.;Newsom,J.R.;and Abel,I.: A Method For Obtaining Reduced Order Control Laws For High Order Systems Using Optimization Techniques. NASA TP-1876,1981.

3. Nissim,E.;and Abel,I.: Development and Application Of An Optimization Procedure For Flutter Suppression Using The Aerodynamic Energy Concept. NASA TP-1137,1978.

4. Mahesh,J.K.;Stone,C.R.;Garrard,W.L.;and Dunn,H.J.:Control Law Synthesis For Flutter Suppression Using Linear Quadratic Gaussian Theory. AIAA J. Guidance and Control, vol. 4, no. 4, July-August 1981,pp.415-422.

5. Nissim,E.;Caspi,A.;and Lottati,I.: Application of the Aerodynamic Energy Concept To Flutter Suppression And Gust Alleviation By Use Of Active Controls. NASA TN D-8212,1976.

6. Nissim,E.: Flutter Suppression Using Active Controls Based On The Concept Of Aerodynamic Energy.NASA TN D-6199.

7. Nissim,E.: Recent Advances In Aerodynamic Energy Concept For Flutter Suppression And Gust Alleviation Using Active Controls.NASA TN D-8519,1977.

8. Adams,W.;and Tiffany,S.: Development Of A Flutter Suppression Control Law By Use Of Linear Quadratic Gaussian And Constrained Optimization Design Techniques. 2nd International Symposium On Aeroelasticity And Structural Dynamics,April 1985,Germany.

9. Burken,J.J.;Alag,G.S.;and Gilyard,G.B.: Aeroelastic Control Of Oblique Wing Aircraft. NASA TM-86808.